Technical Report UNH-OPAL-1999-005

Circulation Variability in the Western Gulf of Maine

W.S. Brown, F. L. Bub and P. Mupparapu

Ocean Process Analysis Laboratory
The Institute for the Study of Earth Oceans and Space
Department of Earth Sciences
University of New Hampshire
Durham, NH 03824

Circulation Variability in the Western Gulf of Maine

W.S. Brown, F. L. Bub, and P. Mupparapu
Ocean Process Analysis Laboratory
The Institute for the Study of Earth Oceans and Space
Department of Earth Sciences
University of New Hampshire
Durham, NH 03824

ABSTRACT

This report describes the basic elements of flow variability in northern Wilkinson Basin at a mooring site located at 42 46.92^{o}N and 69 44.85^{o}W between late August and mid-October 1996. Moored current measurements at 15-minute intervals at a depth of 4m and 15-minutes at 80m, 150m and 220m respectively in 270m of water are statistically-related to the external and internal tidal forcing as well as wind stresses derived from Boston NDBC buoy winds – a proxy regional winds. The series mean currents at each level were somewhat less than 3 cm/s or less and generally directed along the local isobaths toward 220^{o}T; thus defining along-isobath (40^{o}T- 220^{o}T) and across-isobath (310^{o}T-130^{o}T) directions, respectively. Most of the current variance was due to the tides, with M_2 ellipses generally oriented across-isobath. Most of the remaining current variance was surface intensified and partitioned between inertial band (@ 0.57cph) and the 2 to 10 day "weather band". Clockwise inertial oscillations were most prominent at depths of 4m, 150m and 220m respectively for an 8-day following the 17-20 September storm event. The surface-intensified weather band current variability and was most strongly correlated with wind stress normal to it in an Ekman transport sense. The variability in the deeper across-isobath (130^{o}T-310^{o}T) weather band currents were most strongly correlated with the along-isobath (220^{o}T-40^{o}T) wind stress at a lag of 18hr suggesting a compensation for the nearby wind-forced coastal downwelling-upwelling of near-surface currents upper layer currents.

I. Introduction

The Wilkinson Basin is deeper than 270m and one of the deepest basins in the Gulf of Maine - a semi-enclosed marginal sea. Feng (1996), in his study of the wind-induced responses of the coastal western Gulf of Maine during the spring and summer 1994, found a robust Ekman response, with distinctly different structures in the two seasons. His results also suggested that the basin-scale circulation (as opposed to local wind forcing) significantly affected the variability of the deeper offshore parts of the coastal

current regime. This paper focuses on current variability in Wilkinson Basin, with a particular emphasis on the wind-induced response during fall 1996.

In this study, a preliminary statistical analysis of horizontal currents and wind stress components is presented with a conceptual model for the Wilkinson Basin site. In section II, the Wilkinson Basin current measurements and wind observations at the Boston NDBC buoy are described. In section III, the results of a preliminary statistical analysis are presented. In section IV, a summary of results is presented.

II. Description of Data Set

The Fall 1996 (29 August to 17 October) data set consists of horizontal currents and bottom pressure (BP) measured in Wilkinson Basin, the Portland synthetic subsurface pressure (SSP) derived from a sum of the Portland National Ocean Service (NOS) sea level and atmospheric pressure from the Portland National data Buoy Center (NDBC) buoy and winds from the Boston NDBC buoy (located in Figure 1; Table 1). The Wilkinson Basin buoy was moored at a site south of Jeffery's Bank (see Figure 2). The EG&G Vector Averaging Current Meter (VACM) at a depth of 4m sampled every *15 minutes*. Four-minute average currents were measured every *5 minutes* by Alpha-Omega VACMs at 80m, 150m and 220m respectively (Figure 3). A pair of Paroscientific Inc. pressure/temperature sensors mounted on a bottom instrument frame made interval-averaged bottom pressure every *7.5 minutes* near the current meter mooring.

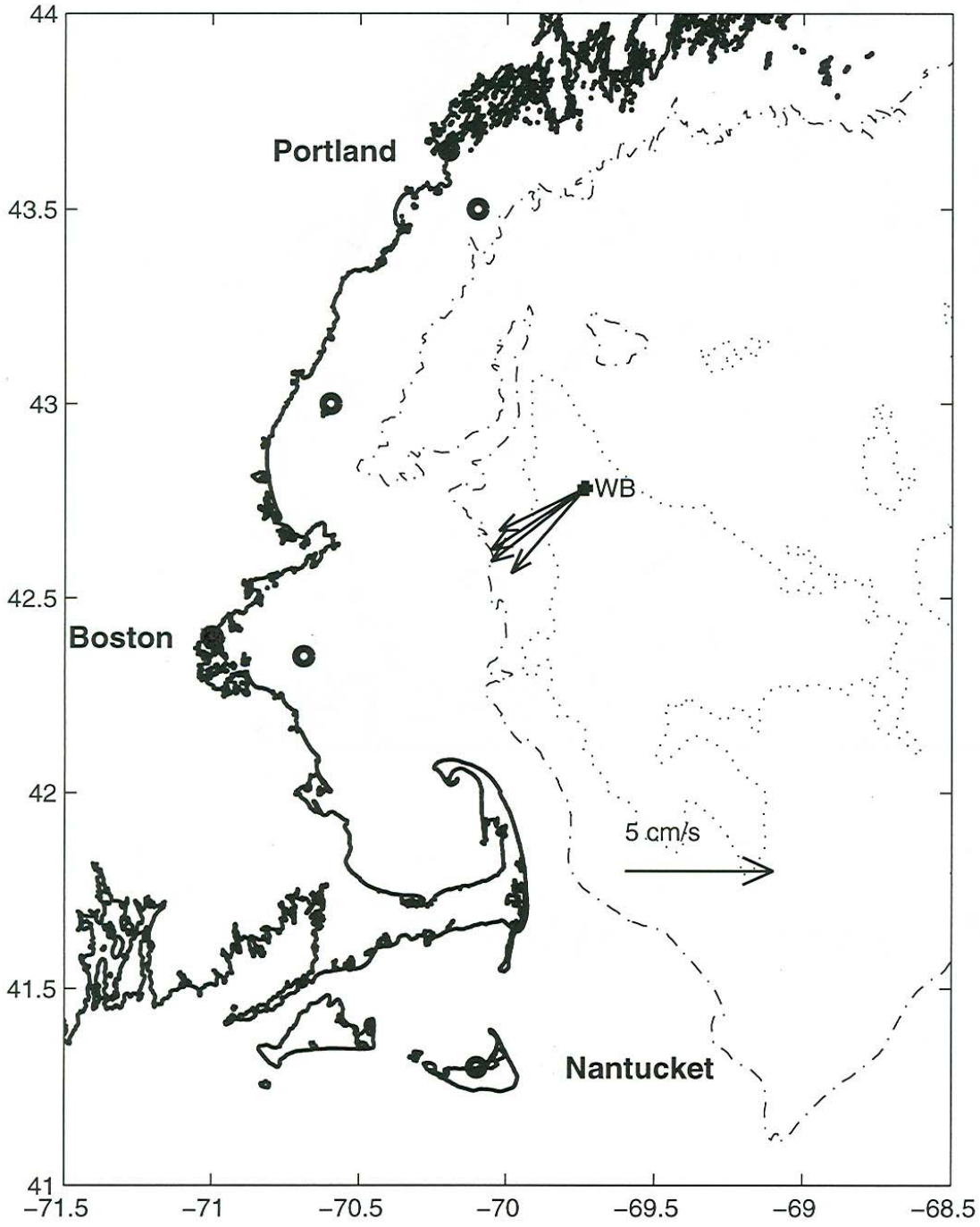

Figure 1 Location map of the August-October 1996 measurements in the Gulf of Maine (Boston and Portland NOS coastal sea level (solid circle); Boston, and Portland NDBC buoy meteorology (open circle); Wilkinson Basin moored currents and bottom pressure (cross). The series mean currents in Wilkinson Basin (WB) are shown.

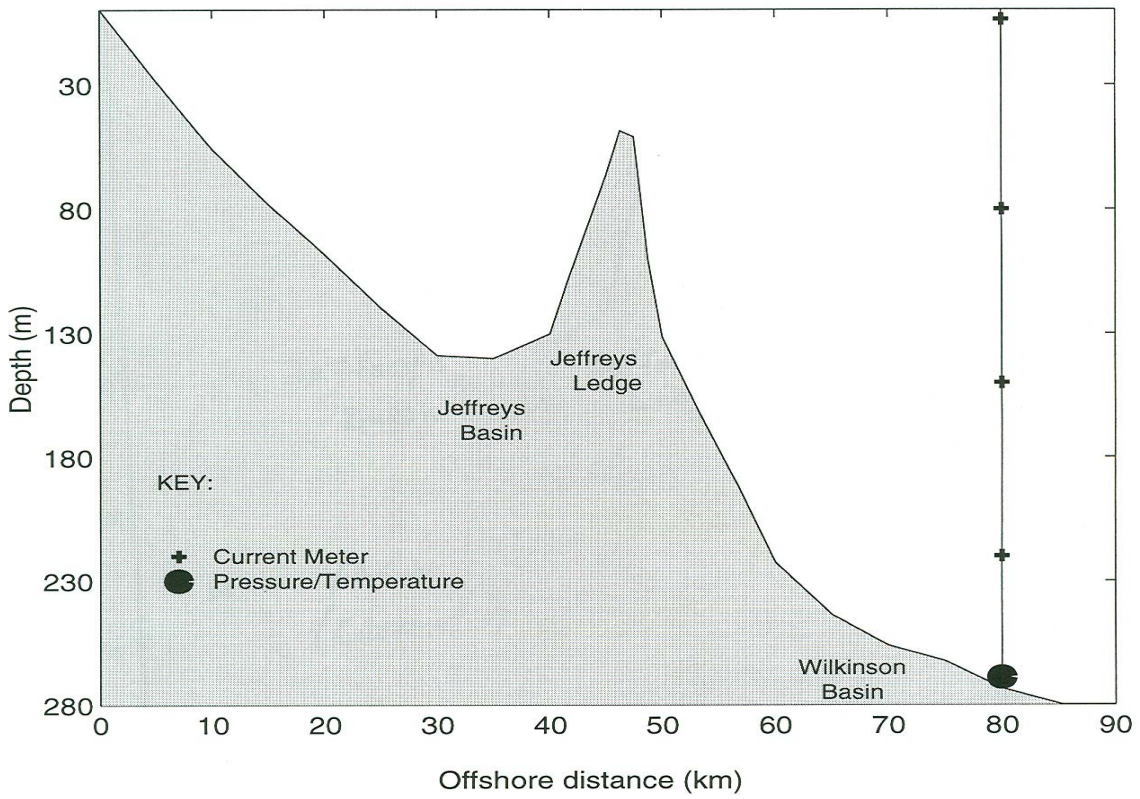

Figure 2 The bathymetry along a north-south transect from Cape Porpoise, ME on the left through Jeffreys Basin to northern Wilkinson Basin – marked by the location of the mooring on the right.

Table 1 Locations of Wilkinson Basin current meter/bottom pressure mooring, NDBC meteorological buoys and NOS coastal sea level stations.

	N LAT deg min	W LON deg min	Depth (m)	Samples per hour	Instrument
METEOROLOGY					
Portland	43 30.0	70 06.0	-5	1	NDBC 44007
Boston	42 24.0	70 42.0	-5	1	NDBC 44013
SEA LEVEL					
Portland	43 39.4	70 14.8	2	1	NOS
Boston	42 21.3	71 03.1	2	1	NOS
CURRENTS/PRESSURES					
Wilkinson Basin Buoy	42 46.92	69 44.85	4	4	EG&G VACM
	(42.782)	(69.748)	80	12	A- Ω VACM
			150	12	A- Ω VACM
			220	12	A- Ω VACM
			270	8	Dual Paroscientific BP/T

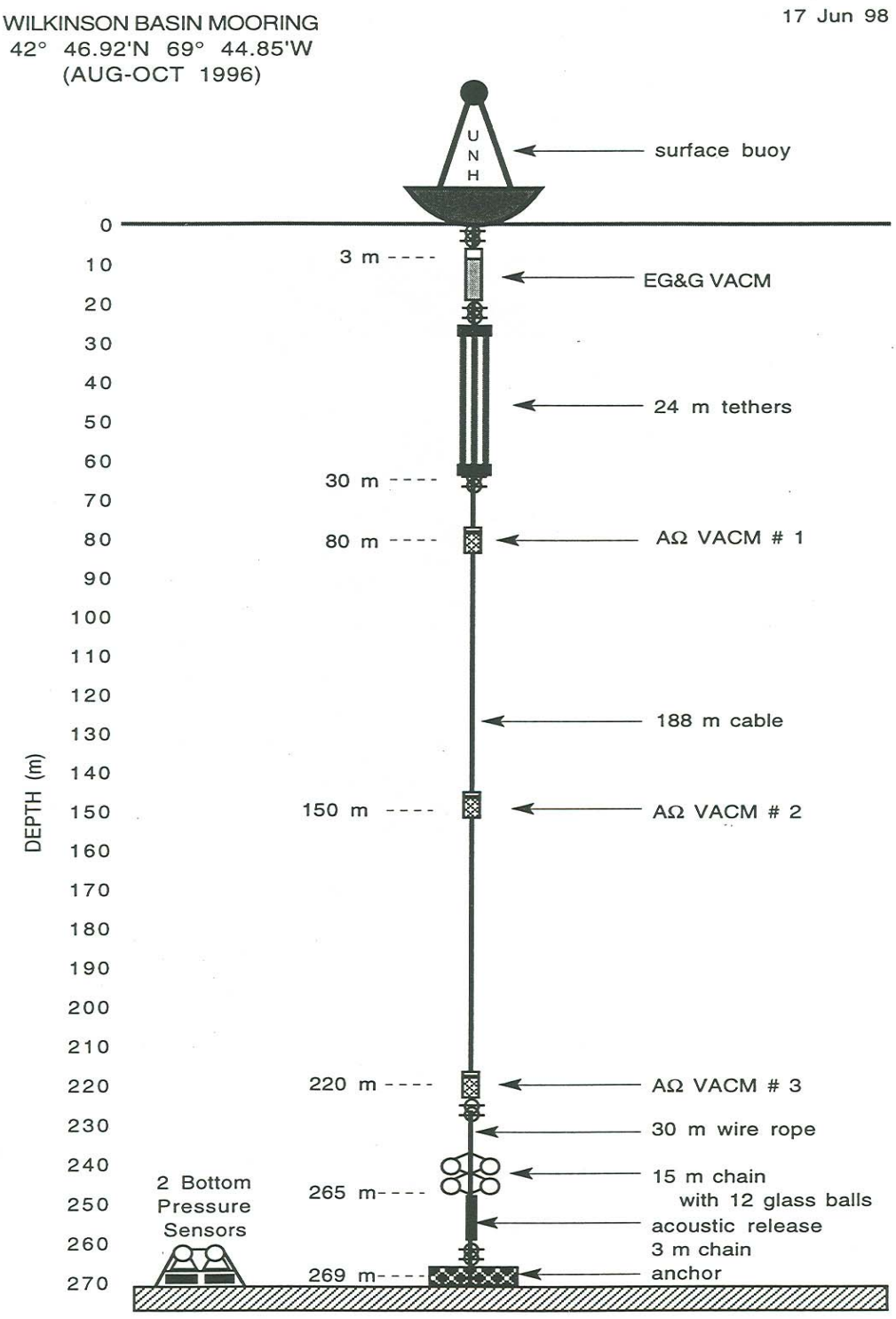

Figure 3 Schematic of the mooring deployed in Wilkinson Basin during Fall 1996.

Hydrography: Hydrographic profiles (see Figure 4) were obtained upon deployment and recovery of the mooring. The strength of the stratification in terms of buoyancy frequency decreased from its probable maximum at about 10m depth in August to its lesser value in October, with its maxima at 40m depth. The upper water column stratification was probably eroded and the mixed layer deepened episodically due to a trio of wind events –augmented by intermittent convective mixing during the study period.

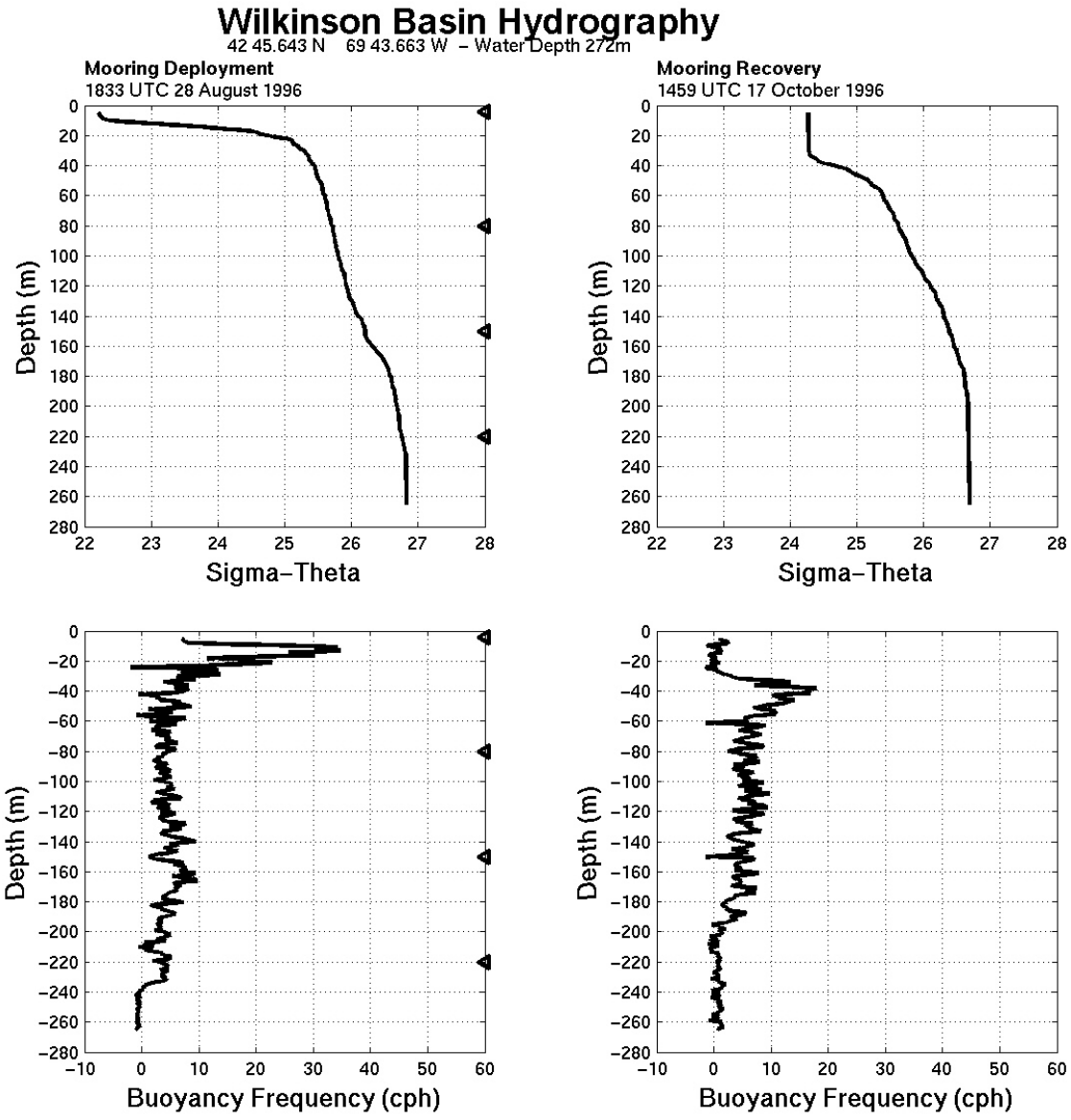

Figure 4 The sigma-theta and buoyancy frequency (cph) profiles derived from CTD measurements of water column properties (left) on 28 August 1996 at the mooring deployment and (right) on 17 October 1996 mooring recovery.

Pressures: The Fall 1996 bottom pressure (BP) records from Wilkinson Basin (see Figure 5), which looked exactly like the Portland synthetic subsurface pressure (SSP) record (not shown), were dominated by the semidiurnal barotropic tide that featured a 1m to 2m tidal sea level variability during neap and spring tides respectively. Thus, as Brown and Irish (1992) have shown, Wilkinson BP is highly coherent with Portland and the other coastal SSP records around the Gulf in the tidal part of the spectrum. The Appendix A harmonic constants clearly document the dominance of the M_2 tidal constituent in the bottom pressure in Wilkinson Basin.

Currents: To better facilitate comparisons, the 15-minute, 4m EG&G VACM current record was interpolated to 5-minute sample rate of the 3 Alpha-Omega current meter records. To more naturally partition the tidal and non-tidal flow components, the standard northward and eastward components were rotated 50° counterclockwise into their respective *across-isobath* (toward 310°T) and *along-isobath* (40°T) current components. The mean currents at the different levels are generally southwestward (about 220°T), approximately parallel to the local bathymetry (i.e. along-isobath) and less than 3 cm/s (see Table 2; Figure 1) in the rotated coordinate system. These mean currents are similar to those from the winter of 1974-75 (Vermersch et al., 1979) and consistent with the idea of steady counterclockwise flow around Wilkinson Basin.

Table 2 The basic statistics of the *5-minute* full, *5-minute* detided and *hourly* along-isobath (40°T) and across-isobath (310°T) currents in Wilkinson Basin between 29 August and 17 October 1996. The statistics of the *hourly* wind stress that was derived from Boston NDBC buoy winds are also included. Note that the hourly data contain most of the current variance.

Current (cm/s)	**Depth (m)**	**5-Minute Mean**	**5-Minute Std Dev**	**5-Minute Detided Std Dev**	**Hourly Mean**	**Hourly Std Dev**
Along-Isobath	4	-2.8	19.6	17.7	-2.8	19.6
	80	-2.9	7.1	6.4	-2.8	7.1
	150	-2.2	9.3	7.8	-2.2	9.2
	220	-2.7	8.9	8.4	-2.8	9.0
Across-Isobath	4	0.0	20.7	17.7	0.0	20.8
	80	0.1	15.9	7.1	0.0	15.8
	150	0.1	12.9	7.6	0.1	12.9
	220	0.1	14.8	8.2	0.1	14.7
Wind Stress (dynes/cm^2)						
Along-Isobath	- 5				-0.19	0.99
Across-Isobath	- 5				-0.26	0.81

The hourly currents in Figure 5, which were derived by low-pass filtering and sub-sampling the 5-minute currents, reveal a flow field that is clearly dominated by the semidiurnal tidal response. The across-isobath tidal currents are the strongest. In addition to the clear tidal signal, the 4m record also exhibits the stronger lower frequency variability, which is primarily due to wind-forcing as will be shown later. It is also possible that some small fraction of the 4m variability may be due to the motion of the surface buoy. The deeper current meters are buffered from the buoy motion by the elastic tethers in the mooring line (see Figure 3).

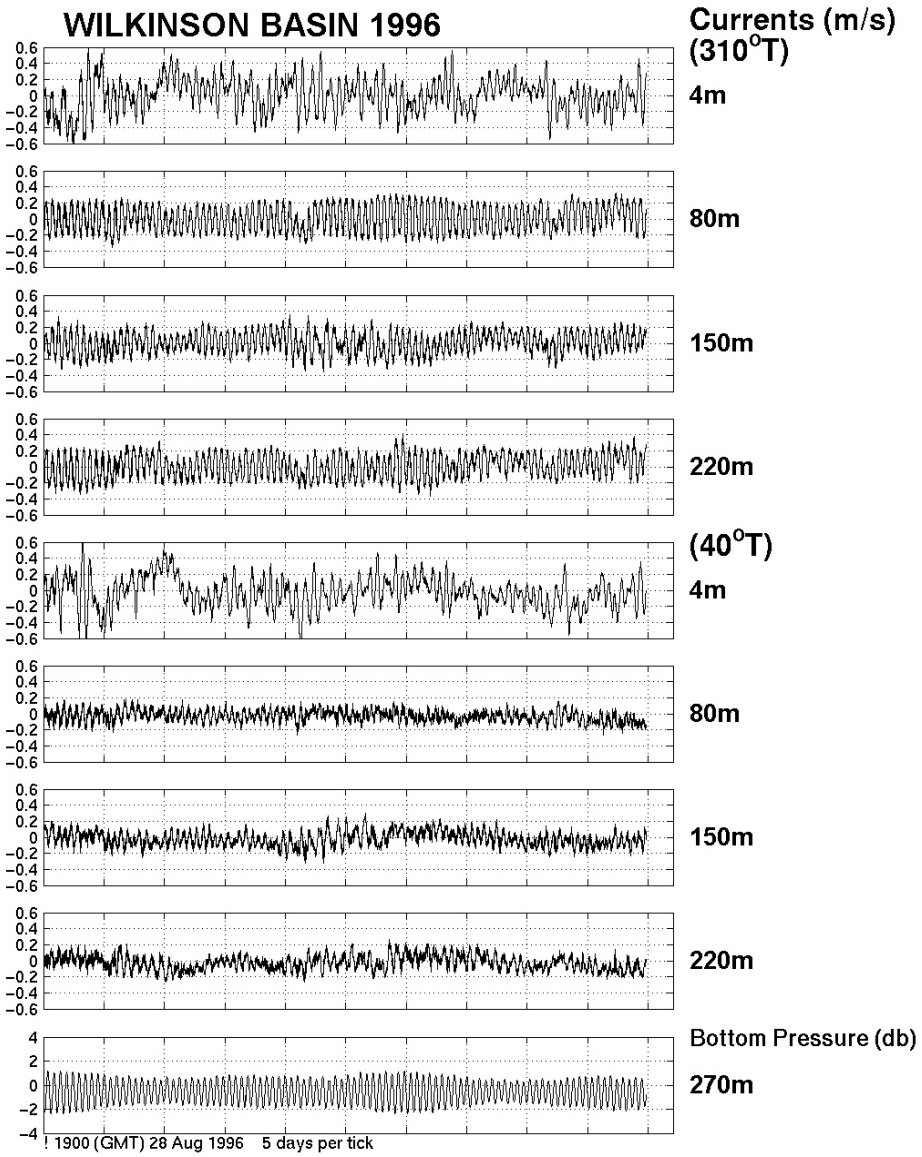

Figure 5 Time series of *hourly* across-isobath (310°T) and along-isobath (40°T) current components at the different depths in Wilkinson Basin between 29 August and 17 October 1996. The bottom pressure record is in the bottom panel.

The spectra of the *full* current records (Figure 6 dotted) are characterized by nearly equally large peaks in the semidiurnal frequency bands (~ 0.08cph) of both the clockwise and anti-clockwise rotary spectra. A harmonic analysis of the records (Appendix B) reveals dominant M_2 semidiurnal tidal currents – all generally consistent with the Moody et al. (1984) results for the region. In particular, (1) the deeper M_2 tidal currents are generally uniformly rectilinear and oriented across-isobath, while (2) the 4m M_2 tidal current amplitude is relatively intensified and its phase significantly different than those of the deeper currents. The difference in surface and deeper M_2 tidal currents is likely due to the presence of a significant internal tide (see below). Because of the tidal similarity of the three deepest currents (located well below the pycnocline; Figure 4), they were averaged to produce an estimate of the local barotropic or external tidal current response (see Appendix B). The estimated external M_2 tidal current ellipse has a major axis amplitude of 0.161 m/s, Greenwich epoch degrees of 10.2, and orientation of 322^{o}T - generally normal to a regional bathymetry that is dominated by the nearby Jeffrey's Bank (see Figure 2).

To better reveal the non-tidal features of the flow, the predicted tidal currents at each level were removed from the current series to obtain the *residual* current records. This process effectively removes the astronomically-driven barotropic tide, as well as that part of the internal tide that is phase-locked (i.e. coherent) to the barotropic tide over the study period. The detiding of the current records is responsible for the large differences in the standard deviations of the basic and detided deeper across-isobath currents (see Table 2). The residual current records (Figure 7) thus feature (1) incoherent semidiurnal tidal variability, (2) intermittent periods of strong inertial motion (e.g. the event about 20 days into the study period), and (3) lower frequency 2-10 day period variability.

The rotary spectra of the *residual* currents (solid, Figure 6) are dominated by the clockwise inertial variability at the local inertial frequency of about 0.057 cph. The residual semidiurnal tidal energy is probably due to that internal tidal variability that is incoherent with the local external or internal tides. The deeper residual 5-minute current spectra decrease relatively smoothly from the inertial frequency to the 6cph Nyquist

frequency. The spectra of the 4m current records begin to roll-off more rapidly at the 2cph Nyquist frequency of basic 15-minute data from which the 5-minute records were interpolated.

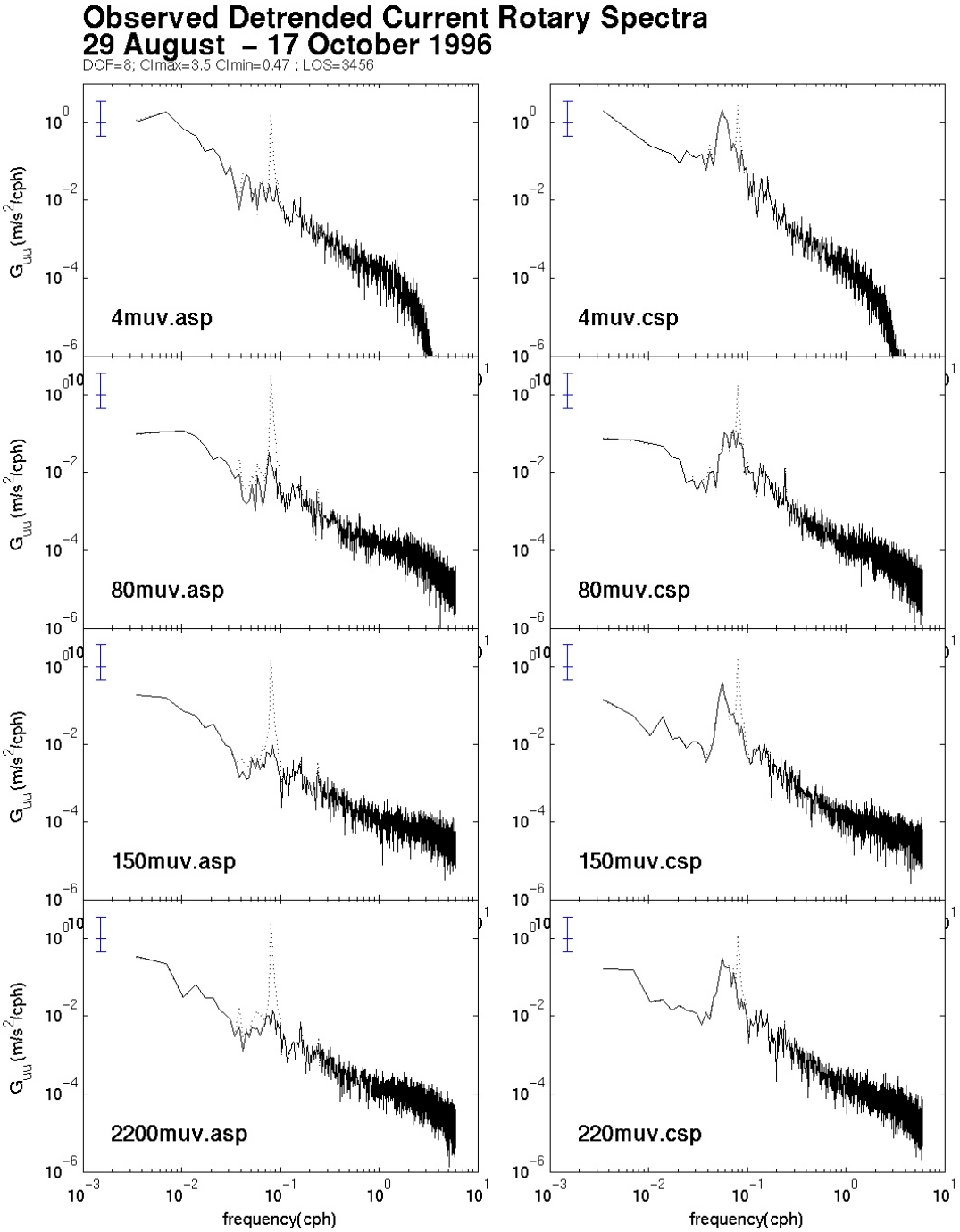

Figure 6 The clockwise (right) and anti-clockwise (left) rotary spectral energy density functions of the *full* (dotted) and *residual* (solid) 5-minute currents in Wilkinson Basin during Fall 1996. The more rapid roll-off of the 4m spectrum at about 2cph is because it is an interpolated record of 15minute samples. The 95% confidence intervals for 8 degrees of freedom (DOF) are indicated.

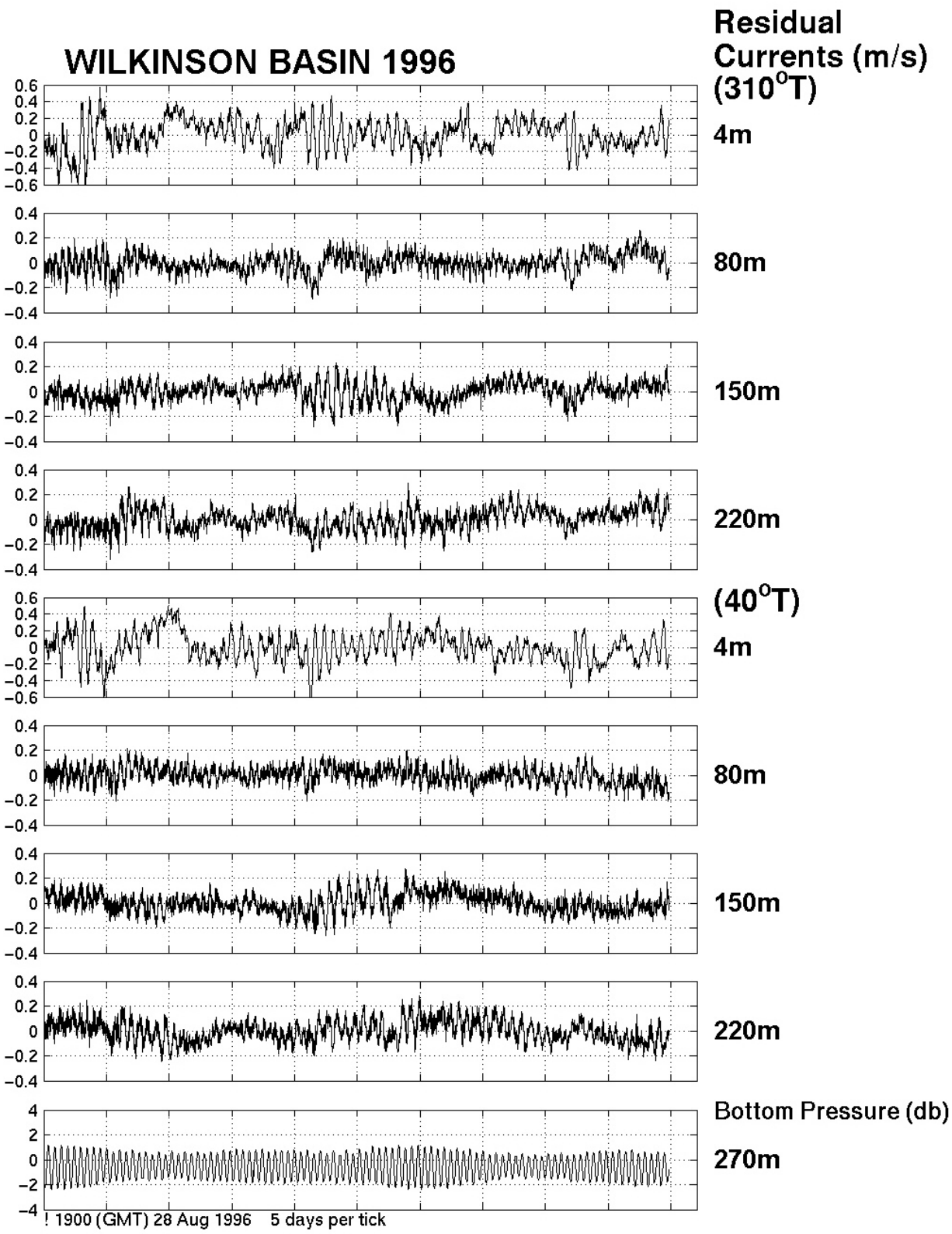

Figure 7 Time series of *5-minute* residual across-isobath (310°T) and along-isobath (40°T) current components at the different depths in Wilkinson Basin between 29 August and 17 October 1996. The bottom pressure record is in the bottom panel.

Inspection of the Figure 6 spectra indicates that a significant part of the total variance of the currents in the 2 to 10 day fluctuation period or "weather band" (i.e. 0.02cph – 0.004 cph). To better focus on the weather band variability, the residual current series were low pass filtered (using a Lanczos filter, with a cut-off frequency of 0.028 cph) and sub-sampled to produce the 6-hourly *subtidal* current records shown in Figure 8.

Visual inspection clearly reveals that the 4m *subtidal* currents were more energetic than the energetically-similar deeper currents (see basic statistics in Table 3a). The statistical information in Table 3b indicates that, with the exception of 80m, the *subtidal* current ellipses are nearly circular at most depths. The near-surface *subtidal* current variability was weakly polarized (major/minor axis ratio R = 1.07), with a slight bias toward 35^{o}T. The 150m and 220m deeper currents were also weakly polarized, with slight biases toward about 80^{o}T. The orientation differences in these cases are insignificant because they are dictated by relatively the small variations in this circularity. The anomalous 80m *subtidal* current variability was more strongly polarized (R = 1.57; 120^{o}T orientation); perhaps due to the reduced inertial flow, with correspondingly greater semidiurnal tidal and weather band variability (see Figure 7).

Note that the *subtidal* current fluctuations at all levels are larger than the series mean currents (particularly at 4m). Thus during the summer-fall transition period, there are frequent current reversals in the 2-10 day weather band.

Wind Stress

Wind stresses were computed using the hourly winds measured at the Boston NDBC buoy and the Large and Pond (1982) bulk formulae. The winds, measured at a height of 5 m, were adjusted to an elevation of 10 m (assuming a "neutrally stable logarithmic wind profile) before computing wind stress components. Most of the wind stress variability was concentrated in the 2 to 10 day "weather band". Thus the low pass filtered wind stress components were also formed using the same filter described earlier. See the vector wind stresses in Figure 8, wind stress statistics in Table 3a, and wind stress ellipse information in Table 3b. The vector wind stress record features three significant

southward events; study period days (a) 2-5; (b) 17-21; and (c) 41-43. These strong "northerlies" wind-forcing events are apparently responsible for producing a very polarized (R = 2.08 in the north-south direction) wind stress ellipse.

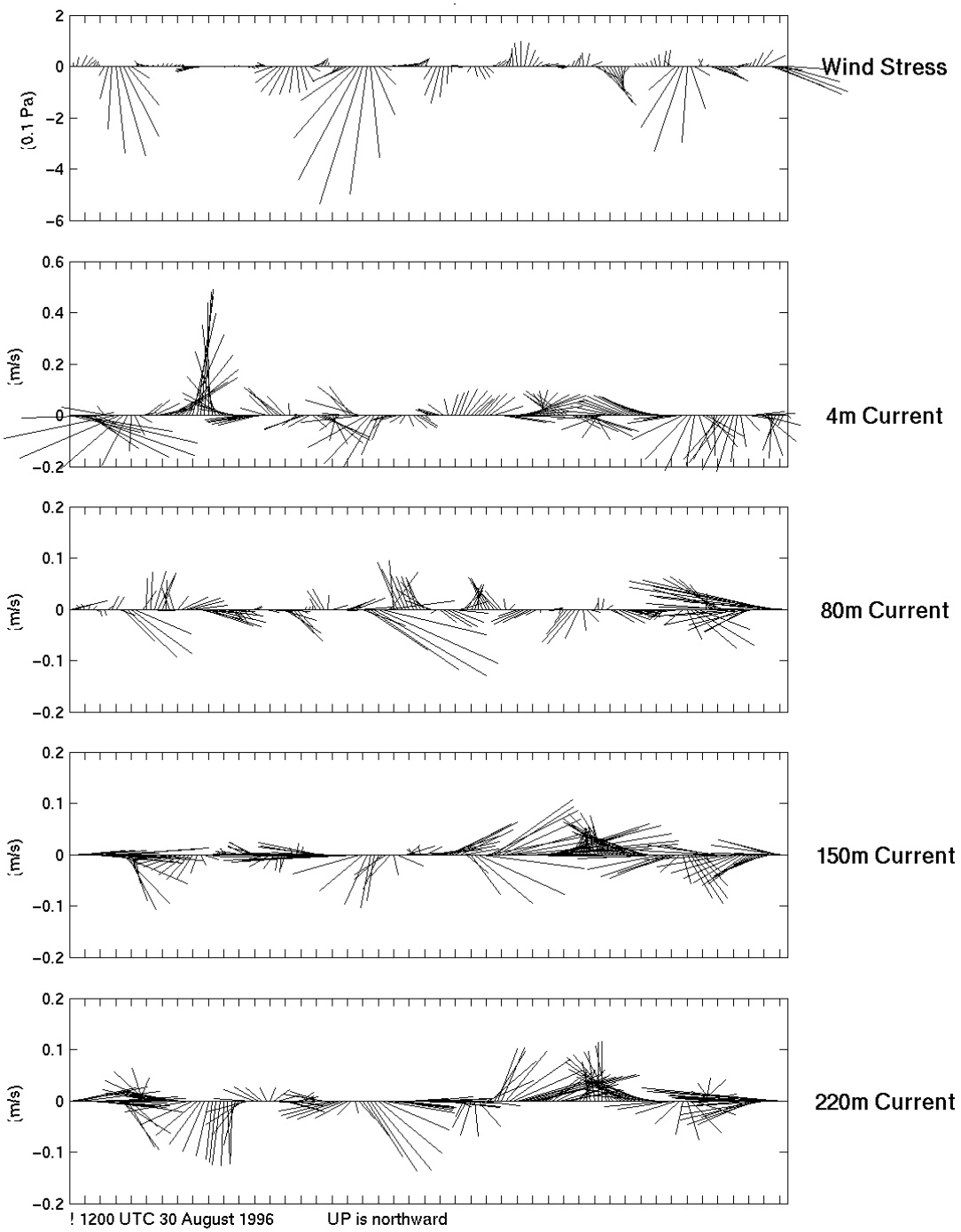

Figure 8 A vector plot of the 6-hrly Fall 1996 subtidal currents in Wilkinson Basin. The corresponding wind stress vectors derived from the Boston NDBC buoy winds are also shown. Note the 3x amplification of the scales for the deeper current records. Upward is northward.

Table 3a The mean values and standard deviations of the *subtidal* along-isobath (40^{o}T) and across-isobath (310^{o}T) currents in Wilkinson Basin and the wind stress derived from Boston NDBC buoy winds between 29 August and 17 October 1996.

Current (cm/s)	**Depth (m)**	**Std Dev**
Along-Isobath	4	12.5
	80	3.1
	150	5.2
	220	5.5
Across-Isobath	4	11.7
	80	4.8
	150	4.7
	220	5.5
Wind Stress ($dynes/cm^2$)		
Along-Isobath	- 5	0.87
Across-Isobath	- 5	0.67

Table 3b *Subtidal* current and wind stress ellipses for Fall 1996. The standard deviations of the *major* and *minor* principal axes, the ratio of major axis to minor axes R and Theta – the orientation of the major axis relative to true north are listed.

Current (cm/s) **Depth** (m)	**Major**	**Minor**	**R**	**Theta** (^{O}T)
4	12.6	11.8	1.07	33
80	4.9	3.1	1.57	126
150	5.7	4.1	1.22	83
220	5.8	5.2	1.12	89
Boston Wind Stress ($dynes/cm^2$)	1.00	0.48	2.08	3

III. Results of Statistical Analysis

The current variability associated with tidal, inertial and wind-driven processes – each their fairly distinct frequency bands - is explored in terms of empirical orthogonal function analysis, which provides insight to correlated structures in suite of data records. On one hand there are the time-domain empirical orthogonal functions (TEOF) are relatively broad-brush in that they partition the total variance - across all frequency bands- of a suite of current records into *correlated* modes (each with their unique structure and an amplitude time series) that are statistically uncorrelated. On the other

hand, there are frequency-domain empirical orthogonal functions (FEOF) that partition the variance within a selected frequency band of a suite of current records into the coherent modes (each with their unique amplitude and phase structure) that are statistically incoherent.

Tidal Band

A TEOF analysis defined the principal structures of the fluctuations of the full 15-minute current records (see Table 4). The *mode-1* across-isobath current TEOF (accounting for 58% of the total variance) exhibits a relatively uniform profile that is consistent with the barotropic tidal results. The energetics of the across-isobath current TEOFs are summarized in terms of the spectral energy density functions of the 3 most energetic TEOF modes shown in Figure 9. The large peak at about 0.08cph in the spectrum of the *mode-1* across-isobath current TEOF amplitude series (58% variance) is consistent with a dominant semidiurnal barotropic tide. The peaks at the semidiurnal frequency harmonics (0.16cph and 0.24cph respectively) are consistent the known nonlinearity Gulf of Maine tidal currents.

The FEOF analysis of the 12.7hr frequency band (containing the 12.4hr M_2 tide) provides special insight to the underlying processes. For example, the *mode-1* FEOF of the across-isobath currents (explaining 98.7% of the variance in the frequency band) has an amplitude profile (Figure 10) that is relatively uniform with depth – consistent with a depth-independent (i.e. barotropic) external tidal currents. However, the *mode-1* across-isobath current FEOF phase profile shows that barotropic currents between 80m and 220m lag the surface current by about a ¼ M_2 tidal cycle. The 12.7hr frequency band, *mode-1* along-isobath current FEOF, while it has some structure, is not nearly as sheared as the corresponding mode-1 TEOF (see Table 4) and appears to be is consistent with a dominant semidiurnal barotropic tide.

In summary, the tidal band statistical results explain a dominant M_2 tidal response that consists of a strong depth-independent profile of nearly rectilinear external tidal currents oriented in the across-isobath direction (~320^{o}T) plus a weaker of surface-intensified (i.e.

depth-dependent or baroclinic) internal tidal currents that are coherent with the external tide. The current shear between 4m and 80m is consistent with the relatively shallow pycnocline (Figure 4). These internal tides are probably generated through the interaction of the barotopic tidal currents with the steep southeast-facing slope of Jeffrey's Bank (see Figure 2). These highly nonlinear internal tidal waves (or sometimes called internal solitons) are known to evolve into packets of higher frequency internal waves that are intermittently present (not shown) in our 5-minute current records.

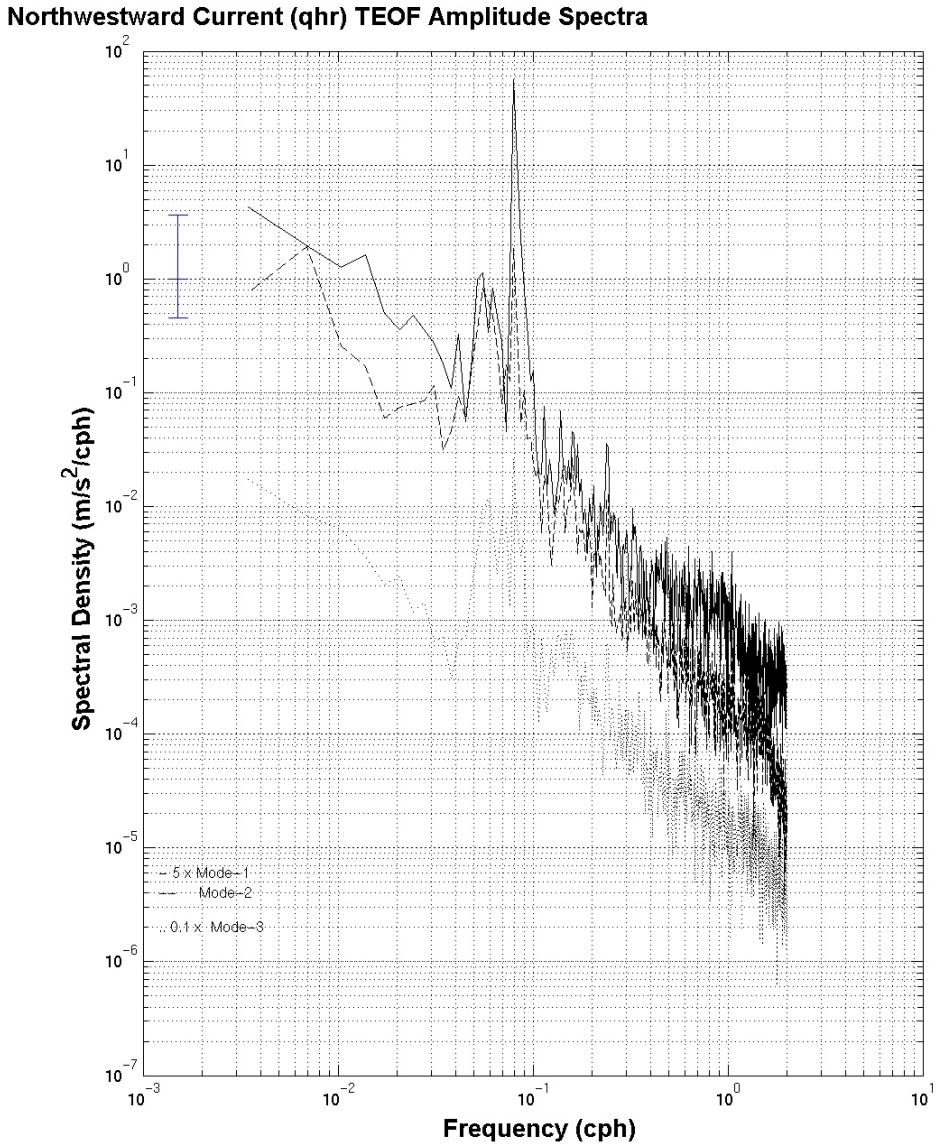

Figure 9 The spectral energy density functions of the three most energetic 15-minute across-isobath current TEOF modes. Modes 1 (5x___) and 3 (0.1x -.-.-) have been adjusted vertically relative to an unmodified mode 2 (----) for clarity. The 95% confidence intervals are indicated.

Table 4 The TEOF structures (m/sec) of the first three modes of the 15-minute along-isobath (40°T) and across-isobath (310°T) currents for the Wilkinson mooring site for Fall 1996. The % of the total variance of the time series explained by each mode is indicated.

Depth (m)	**40°T Mode-1** (65%)	**40°T Mode-2** (19%)	**40°T Mode-3** (9%)	**310°T Mode-1** (58%)	**310°T Mode-2** (32%)	**310°T Mode-3** (6%)
4	0.196	0.009	0.000	0.141	0.152	-0.001
80	0.015	-0.008	-0.041	0.131	-0.067	-0.054
150	0.018	-0.075	0.043	0.100	-0.046	0.058
220	0.004	-0.072	-0.040	0.122	-0.066	0.012

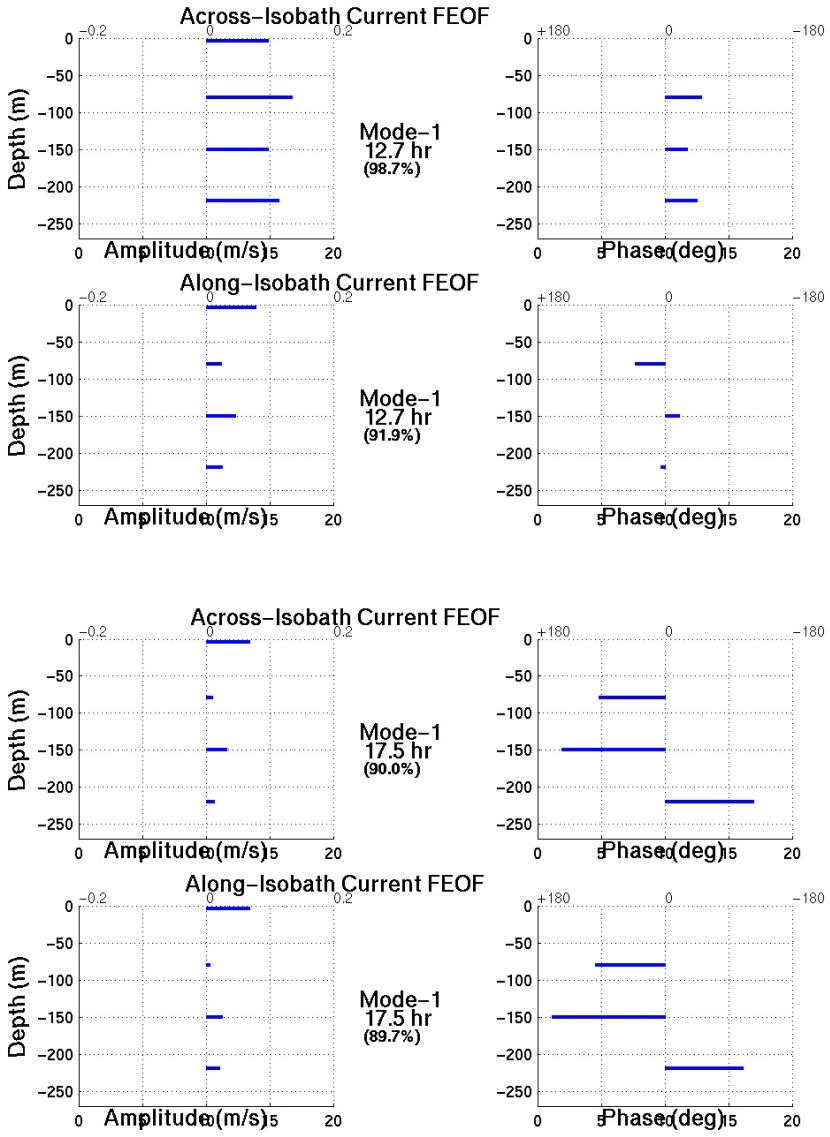

Figure 10 The mode-1 FEOF amplitude (left) and phase (right) profiles of the across-isobath and along-isobath current components in the (upper) 12.7hr semidiurnal tidal band and (lower) 17.5hr inertial band. The phases are referenced to the 4m current. The % variance of the mode is indicated.

The Inertial Band

The spectrum of the *mode-2* across-isobath current TEOF (32% variance) has a significant peak at the local inertial frequency band (near 0.57cph). To explore the statistical structures that non-tidal variability, we conducted a TEOF analysis of the *residual* (non-tidal) 15-minute current records (see Table 5). We note that both the *mode-1 residual* across-isobath current (65% of the total variance) and the *mode-1* residual along-isobath current TEOF (66% of the variance) (see Table 5), are **surface-intensified.** The spectrum of the mode-1 *residual* current TEOF in Figure 11 is dominated by the inertial frequency band peak.

Table 5 The TEOF structures (m/sec) of the first three modes of the *residual* 15-minute along-isobath (40^oT) and across-isobath (310^oT) currents for the Wilkinson mooring site during Fall 1996. The % of the total variance of the time series explained by each mode is indicated.

Depth (m)	**40^oT Mode-1** (66%)	**40^oT Mode-2** (17%)	**40^oT Mode-3** (9%)	**310^oT Mode-1** (65%)	**310^oT Mode-2** (17%)	**310^oT Mode-3** (10%)
4	0.177	-0.009	-0.000	0.176	-0.011	-0.002
80	0.007	0.001	0.017	-0.005	-0.032	0.052
150	-0.009	-0.056	-0.050	-0.016	-0.044	- 0.048
220	-0.014	-0.071	0.040	-0.015	-0.070	0.007

The inertial frequency band FEOFs of both the across- and along-isobath currents show the surface current amplitude intensification (see 17.5hr FEOF in Figure 10), but more importantly a strong depth-dependent phase profile, in which the deeper currents lead the shallower currents. The phase lead is extreme; e.g. the 220m current components leads the 4m current by ~ 235^o (equivalent to the plotted 125^o phase "lag") and decreases nearly linearly going up in the water column. The rotary spectra of the inertial band currents indicate the expected clockwise rotary motion at each depth. For inertial motion, the indicated upward phase velocity is equivalent the downward group velocity/energy transmission that would be expected for meteorologically forced inertial oscillations.

In summary, we conclude the inertial frequency band residual currents are probably due to the episodic wind-forced inertial flow response of the study site. Of course, the inertial

oscillations are the initial response mode of the ocean to strong wind-forcing events that occur with a frequency of 2 to 10 days – the focus of the next section.

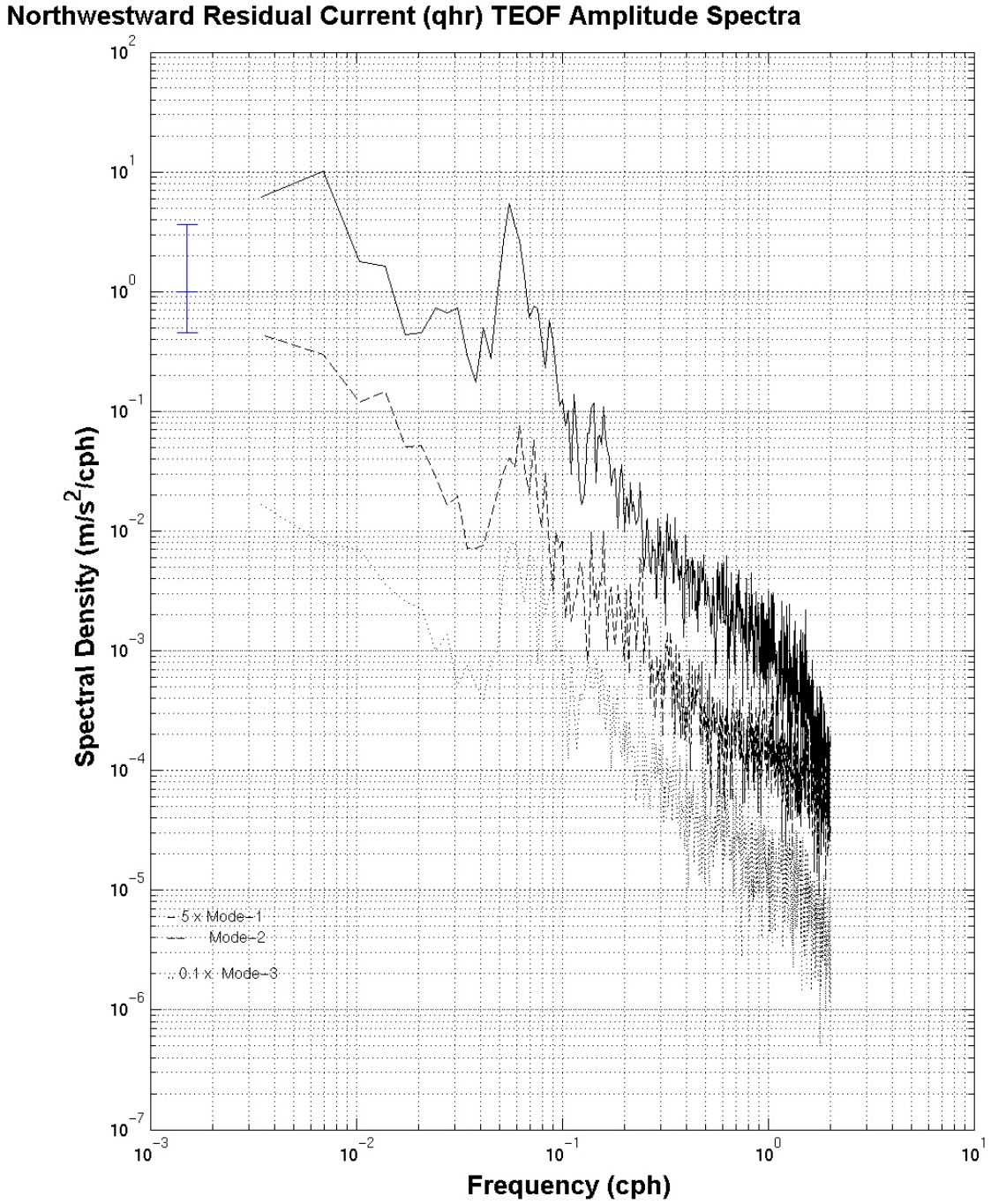

Figure 11 The spectral energy density functions of the three most energetic *residual* across-isobath current TEOF modes. Modes 1 (5x___) and 3 (0.1x -.-.-) have been adjusted vertically relative to an unmodified mode 2 (----) for clarity. The 95% confidence intervals are indicated.

The Wind-Forced Band

The statistical analyses of the *subtidal* along-isobath and across-isobath currents fluctuations, with periods greater than 36 hours, emphasize the non-inertial frequency wind-forced response. The *subtidal* current ellipses (Table 3b) are surface-intensified with orientations, while varying between 33°T and 128°T, tend to be east-west in contrast to the north-south orientation of the wind stress ellipse.

The structures of both the *mode-1 subtidal* along-isobath current TEOF (72% of the total variance) and along-isobath current *mode-1* TEOF (65% of the total variance) are surface-intensified (see Table 6) - suggesting a wind-forced response. A cross-correlation analysis (see Table 7) shows that both components are consistent with locally-forced Ekman transport dynamics; that is flow to the right of the wind stress. Specifically, the *subtidal* along-isobath current *mode-1* TEOF is most correlated (0.64; 0hr time lag) with the 310°T Boston wind stress; while similarly the *subtidal* across-isobath current *mode-1* TEOF was significantly correlated (0.47; -6hr time lag) with the 220°T Boston wind stress.

The less energetic *mode-2 subtidal* across-isobath current TEOF (explaining 25% of the total variance) (Table 6) is dominated by southeastward (130°T) currents between 80m and 220m depth; and most robustly correlated with 250°T Boston wind stress (0.59; see Table 7) at a lag of 18hr. The inertial period delay suggests that this mode may describe a seaward flow that compensates for a nearby coastal wind stress-induced downwelling. It is interesting that the *mode-2 subtidal* along-isobath current TEOF (21% of the variance) (Table 6), with a structure similar to the across-isobath current mode, is not statistically correlated with wind stress at all. Thus the geography probably plays a part in the dynamics.

Table 6 The TEOF structures (m/sec) of the first three modes of the *subtidal* along-isobath (40°T) and across-isobath (310°T) currents for the Wilkinson mooring site for Fall 1996. The % of the total variance of the time series explained by each mode is indicated.

Depth (m)	40°T Mode-1 (72%)	40°T Mode-2 (21%)	40°T Mode-3 (4%)	310°T Mode-1 (65%)	310°T Mode-2 (25%)	310°T Mode-3 (7%)
4	0.125	0.010	-0.001	0.117	-0.004	-0.005
80	0.009	-0.004	0.028	-0.015	-0.031	-0.034
150	0.018	-0.044	-0.010	0.006	-0.039	0.019
220	0.008	-0.052	0.006	-0.004	-0.053	0.006

Table 7 Maximum cross-correlations (C_{max}) and time lags (T_{max}; + => stress leads current) between wind stresses in different directions (Theta) and the TEOF amplitude series of the *subtidal* along-isobath (40°T) and across-isobath (310°T) currents. NR indicates statistically *insignificant* correlations < 0.40.

Along-Isobath (40°T) **Current TEOF**	**Theta** (°T)	$\mathbf{C_{max}}$	$\mathbf{T_{max}}$ (hr)
Mode 1	310	0.64	0
Mode 2	NR	NR	NR
Mode 3	220	0.58	48
Across-Isobath (310°T) **Current TEOF**			
Mode 1	220	0.47	- 6
Mode 2	250	0.59	18
Mode 3	220	0.53	24

IV. Summary of Results

This report describes the basic elements of flow variability in northern Wilkinson Basin at a mooring site located at 42 46.92°N and 69 44.85°W between late August and mid-October 1996. Moored current measurements at 15-minute intervals at a depth of 4m and 15-minutes at 80m, 150m and 220m respectively in 270m of water are statistically-related to the external and internal tidal forcing as well as wind stresses derived from Boston NDBC buoy winds – a proxy regional winds. The series mean currents at each level were somewhat less than 3 cm/s or less and generally directed along the local isobaths toward 220°T – consistent with the winter measurements on Cashes Ledge to the northeast by Vermersch et al. (1979). Most of the current variance was due to the tides, with M_2 ellipses generally oriented across-isobath. With the mean and tidal flow variability defining preferred along-isobath (40°T- 220°T) and across-isobath (310°T-130°T) directions, subsequent analysis focused on currents in the rotated coordinate system. Most of the remaining current variance was surface intensified and partitioned

between inertial band (@ 0.57cph) and the 2 to 10 day "weather band". Clockwise inertial oscillations were most prominent at depths of 4m, 150m and 220m respectively for an 8-day following the 17-20 September storm event. The surface-intensified weather band current variability and was most strongly correlated with wind stress normal to it in an Ekman transport sense. The variability in the deeper across-isobath (130^oT-310^oT) weather band currents were most strongly correlated with the along-isobath (220^oT-40^oT) wind stress at a lag of 18hr suggesting a compensation for the nearby wind-forced coastal downwelling-upwelling of near-surface currents upper layer currents.

APPENDIX A

The harmonic constants of the 25 principal tidal constituents based on an analysis of the Fall 1996 bottom pressure in Wilkinson Basin**.** The tidal constituent characteristics are given in terms of the (a) amplitudes (b) Greenwich epoch and (c) local epoch. The uncertainty limits are given for each quantity except the higher harmonics.

Con	H(m)	G(deg)	κ(deg)
M_2	1.200 +±0.019	108.3 ± 0.8	328.8 ± 0.8
N_2	0.275 +±0.019	77.7 ± 3.4	298.2 ± 3.4
S_2	0.177 +±0.019	138.7 ± 5.3	359.2 ± 5.3
0_1	0.113 ±0.019	190.2 ± 8.8	120.4 ± 8.8
K_1	0.078 ±0.018	223.9 ± 13.1	154.2 ± 13.1
K_2	0.048 ±0.019	141.2 ± 21.4	1.7 ± 21.4
L_2	0.039 ±0.018	138.9 ± 26.0	359.4 ± 26.0
(2N)	0.037 ±0.018	47.1 ± 28.6	267.6 ± 28.6
R_2	0.001 ±0.002	139.9 ±105.5	0.4 ±105.5
T_2	0.010 ±0.012	137.5 ± 78.9	358.0 ± 78.9
λ	0.008 ±0.011	122.4 ± 86.4	342.9 ± 86.4
μ_2	0.029 ±0.018	77.9 ± 36.2	298.4 ± 36.2
ν_2	0.053 ±0.019	81.8 ± 19.7	302.3 ± 19.7
J_1	0.009 ±0.011	62.1 ± 84.3	352.4 ± 84.3
M_1	0.009 ±0.012	27.0 ± 82.7	317.3 ± 82.7
00_1	0.005 ±0.007	257.7 ± 98.1	187.9 ± 98.1
P_1	0.026 ±0.017	248.4 ± 40.0	178.6 ± 40.0
Q_1	0.022 ±0.017	352.0 ± 46.4	282.2 ± 46.4
(2Q)	0.003 ±0.004	153.8 ±104.0	84.1 ±104.0
ρ_1	0.004 ±0.006	330.1 ± 99.6	260.4 ± 99.6
M_4	0.013	355.5	76.5
M_6	0.003	218.4	159.9
M_8	0.001	196.0	358.0
S_4	0.002	33.9	114.9
S_6	0.002	315.1	256.6

APPENDIX B

The harmonic constants of the 5 principal tidal constituents based on the 49 day Fall 1996 current records (plus 80m-220m average currents) from Wilkinson Basin; amplitude H; phase in Greenwich and local epoch The ellipse characteristics are given in terms of the (a) major and minor axes half-amplitudes, (b) orientation of the major axis relative to true north, and (c) the Greenwich phase of the maximum velocity.

		Eastward			Northward			Ellipse			
Depth (m)		**H (m/s)**	**Phase (G^o)**	**Phase (κ^o)**	**H (m/s)**	**Phase (G^o)**	**Phase (κ^o)**	**Maj (m/s)**	**Min (m/s)**	**Phase (G^o)**	**Orien (^oT)**
4	M_2	0.043	128.26	348.76	0.168	334.79	195.29	0.173	-0.019	153.3	347
	N_2	0.008	65.22	285.72	0.030	270.18	130.68	0.031	-0.003	88.7	346
	S_2	0.019	132.97	353.47	0.031	21.00	241.50	0.032	-0.017	11.3	342
	O_1	0.013	70.76	1.01	0.016	354.55	284.80	0.017	-0.012	11.6	337
	K_1	0.045	268.67	198.92	0.013	162.72	92.97	0.045	-0.013	90.1	275
80	M_2	0.137	210.00	70.50	0.128	8.02	228.52	0.184	0.036	19.8	313
	N_2	0.025	125.96	346.46	0.039	344.82	205.32	0.044	-0.014	154.9	331
	S_2	0.016	259.56	120.06	0.013	31.03	251.53	0.019	0.008	61.8	306
	O_1	0.008	238.55	168.80	0.016	34.29	324.54	0.018	0.003	38.8	335
	K_1	0.006	269.96	200.21	0.016	100.76	31.01	0.017	-0.001	99.5	340
150	M_2	0.064	180.08	40.58	0.136	359.40	219.90	0.150	0.001	179.5	335
	N_2	0.016	191.53	52.03	0.016	309.09	169.59	0.019	0.012	163.5	311
	S_2	0.018	215.07	75.57	0.019	53.09	273.59	0.026	-0.004	44.8	317
	O_1	0.011	270.15	200.40	0.002	290.77	221. 02	0.011	0.001	90.9	80
	K_1	0.007	333.31	263.56	0.009	357.06	287.31	0.011	0.002	169.2	35
220	M_2	0.106	203. 12	63.62	0.122	3.54	224.04	0.159	0.027	11.9	319
	N_2	0.022	151.81	12.31	0.030	330.51	191.01	0.037	0.000	151.0	324
	S_2	0.018	203.73	64.23	0.027	42.64	263.14	0.032	-0.005	36.8	326
	O_1	0.009	273.83	204.08	0.006	33.59	323.84	0.010	0.005	80.0	296
	K_1	0.006	40.04	330.29	0.010	85.34	15.59	0.011	0.004	75.7	26
AVE	M_2	0.101	201. 42	61.92	0.128	3.43	223.93	0.161	0.025	10.2	322
80m	N_2	0.020	150.74	11.24	0.026	332.77	193.27	0.032	-0.001	152.0	323
to	S_2	0.016	230.93	91.43	0.019	41.39	261.89	0.025	0.002	45.3	320
220m	O_1	0.008	277.30	207.55	0.007	34.05	324.30	0.009	0.006	67.7	313
	K_1	0.003	348.51	278.76	0.007	83.29	13.54	0.007	0.003	84.1	358

ACKNOWLEDGEMENTS

This research was supported by the Regional Marine Research Program under NOAA grant NA56RM0555, University of Maine subcontract UM-S277; UNH/UMaine Sea Grant under NOAA grant NA56RG0159 and University of Maine subcontracts UM-S221 and UM-S304.

REFERENCES

Brown, W.S., and Irish, J.D., 1992. The annual evolution of geostrophic flow in the Gulf of Maine: 1986-1987. *J. Phys. Ocean*ogr., 22, 445-473.

Feng, H., 1996. "Wind-induced responses of the western coastal Gulf of Maine during spring and summer 1994". M. S. Thesis, Ocean Process Analysis Laboratory, Department of Earth Sciences, University of New Hampshire, Durham, NH.

Large, W.S., and S. Pond, 1981. Open ocean momentum flux measurements in moderate to strong winds*, J. Phys. Oceanogr*., 11, 394-410.

Moody, J., B. Butman, R.C. Beardsley, W.S. Brown**,** W. Boicourt, P. Daifuku, J.D. Irish, D.A. Mayer, H.E. Mofjeld, B. Petrie, S. Ramp, D. Smith and W.R. Wright, 1984."Atlas of Tidal Elevation and Current Observations on the Northeast American Continental Shelf and Slope," *U.S. Geological Survey Bulletin No. 1611*, U.S. Government Printing Office, pp. 122.

Vermersch, J.A., R.C. Beardsley and W.S. Brown, 1979. "Winter Circulation in the Western Gulf of Maine: Part 2, Current and Pressure Observations," *Journal of Physical Oceanography,* Vol. 9, 768-764, (WHOI Contribution 4245)